

# **ASSESSMENT OF THE PERFORMANCE OF COMMON 2-D RESISTIVITY ARRAYS**

**AMSIR**

**UNIVERSITI SAINS MALAYSIA**

**2018**

# **ASSESSMENT OF THE PERFORMANCE OF COMMON 2-D RESISTIVITY ARRAYS**

by

**AMSIR**

**Thesis submitted in fulfillment of the requirements  
for the degree of  
Master of Science**

**May 2018**

## ACKNOWLEDGEMENT

In the name of Allah, The Beneficent, The Merciful

Alhamdulillah, I would like to thank Allah the Almighty for His blessing and mercy. My sincere gratitude goes to my supervisor, Associate Professor Dr. Rosli Saad for his supervision, support and encouragement towards the completion of this thesis, and also for Dr. Andy Anderson Bery and Dr. Nordiana Binti Mohd Muztaza for their support and advices during my study. I would like to thank the financial support from Center of Global Archaeological Research (CGAR) Universiti Sains Malaysia (USM).

My gratitude is also addressed to my beloved parents, Muhammad Taib and Chamsiah for their love and prays for me and to my brother and sister, Fauzi M Taib and Nalirah M Taib for their support.

I would like to thank all my colleagues in the “Team Geophysics” group for the friendship, support and the brilliant discussion until completion of this thesis. Also thanks to lecturers, staffs and technicians in School of Physics, USM who help me directly or indirectly throughout the research.

## TABLE OF CONTENTS

Acknowledgement	ii
Table of Contents	iii
List of Tables	vii
List of Figures	xii
List of Symbols	xvi
List of Abbreviations	xvii
Abstrak	xviii
Abstract	xx

### CHAPTER 1 : INTRODUCTION

1.0 Background	1
1.1 Problems statements	2
1.2 Research objectives	2
1.3 Scope of study	3
1.4 Significant and novelty	3
1.5 Thesis layout	4

### CHAPTER 2 : LITERATURE REVIEW

2.0 Introduction	5
2.1 Previous works	5
2.2 Summary	17

## **CHAPTER 3 : METHODOLOGY**

3.0	Introduction	19
3.1	Electrical resistivity method	19
3.2	Electrical resistivity	21
3.3	Electrode array	26
3.3.1	Wenner array	27
3.3.2	Wenner-Schlumberger array	28
3.3.3	Dipole-dipole array	29
3.3.4	Pole-dipole array	30
3.4	Depth of investigation	32
3.5	Sensitivity index	34
3.6	Research flowchart	34
3.7	Synthetic model	37
3.7.1	Single block model	38
3.7.2	Two blocks model	38
3.7.3	Vertical dyke model	39
3.7.4	Contact vertical zone model	40
3.7.5	Fault model	40
3.8	Field study	41
3.9	Summary	43

## **CHAPTER 4 : RESULT AND DISCUSSION**

4.0	Introduction	44
4.1	2-D resistivity inversion for synthetic model	44
4.1.1	Single block model	44

4.1.2	Two blocks model	50
4.1.3	Contact vertical zone model	56
4.1.4	Vertical dyke model	62
4.1.5	Fault model	68
4.2	Assessment of the performance for synthetic model	73
4.2.1	PDP:WNR array	73
4.2.2	PDP:WSCH array	77
4.2.3	PDP:DPD array	81
4.2.4	DPD:WNR array	86
4.2.5	DPD:WSCH array	90
4.2.6	WSCH:WNR array	93
4.3	2-D resistivity inversion for field survey	97
4.4	Assessment of the performance for field study	101
4.4.1	PDP:WNR array	101
4.4.2	PDP:WSCH array	104
4.4.3	PDP:DPD array	108
4.4.4	DPD:WNR array	113
4.4.5	DPD:WSCH array	116
4.4.6	WSCH:WNR array	120
4.5	Discussion	123
4.6	Summary	127
 <b>CHAPTER 5 : CONCLUSION AND RECOMMENDATIONS</b>		
5.0	Conclusion	129
5.1	Recommendation	131

**REFERENCES**

132

**APPENDICES**

**LIST OF PUBLICATION**

## LIST OF TABLES

		<b>Page</b>
Table 3.1	Depth of investigation, $Z_e$ , spacing, $a$ and total length, $L$ for different arrays (Edward, 1977)	33
Table 3.2	Assessment of the performance for penetration depth worksheet	36
Table 3.3	Assessment of the performance for horizontal / vertical data coverage worksheet	37
Table 3.4	Assessment of the performance for sensitivity index worksheet	37
Table 4.1	Assessment of the comparison performance of penetration depth for PDP:WNR array based on all synthetic models with electrode spacing of 1 m	74
Table 4.2	Assessment of the comparison performance of horizontal data coverage for PDP:WNR array based on all synthetic models with electrode spacing of 1 m	75
Table 4.3	Assessment of the comparison performance of vertical data coverage for PDP:WNR array based on all synthetic models with electrode spacing of 1 m	75
Table 4.4	Assessment of the comparison performance of sensitivity index for PDP:WNR array based on all synthetic models with electrode spacing of 1 m	77
Table 4.5	Assessment of the comparison performance of penetration depth for PDP:WSCH array based on all synthetic models with electrode spacing of 1 m	78
Table 4.6	Assessment of the comparison performance of horizontal data coverage for PDP:WSCH array based on all synthetic models with electrode spacing of 1 m	79
Table 4.7	Assessment of the comparison performance of vertical data coverage for PDP:WSCH array based on all synthetic models with electrode spacing of 1 m	79
Table 4.8	Assessment of the comparison performance of sensitivity index for PDP:WSCH array based on all synthetic models with electrode spacing of 1 m	80



Table 4.9	Assessment of the comparison performance of penetration depth for PDP:DPD array based on all synthetic models with electrode spacing of 1 m	81
Table 4.10	Assessment of the comparison performance of horizontal data coverage for PDP:DPD array based on all synthetic models with electrode spacing of 1 m	82
Table 4.11	Assessment of the comparison performance of vertical data coverage for PDP:DPD array based on all synthetic models with electrode spacing of 1 m	83
Table 4.12	Assessment of the comparison performance of sensitivity index for PDP:DPD array based on all synthetic models with electrode spacing of 1 m	85
Table 4.13	Assessment of the comparison performance of penetration depth for DPD:WNR array based on all synthetic models with electrode spacing of 1 m	86
Table 4.14	Assessment of the comparison performance of horizontal data coverage for DPD:WNR array based on all synthetic models with electrode spacing of 1 m	87
Table 4.15	Assessment of the comparison performance of vertical data coverage for DPD:WNR array based on all synthetic models with electrode spacing of 1 m	88
Table 4.16	Assessment of the comparison performance of sensitivity index for DPD:WNR array based on all synthetic models with electrode spacing of 1 m	89
Table 4.17	Assessment of the comparison performance of penetration depth for DPD:WSCH array based on all synthetic models with electrode spacing of 1 m	90
Table 4.18	Assessment of the comparison performance of horizontal data coverage for DPD:WSCH array based on all synthetic models with electrode spacing of 1 m	91
Table 4.19	Assessment of the comparison performance of vertical data coverage for DPD:WSCH array based on all synthetic models with electrode spacing of 1 m	92
Table 4.20	Assessment of the comparison performance of sensitivity index for DPD:WSCH array based on all synthetic models with electrode spacing of 1 m	93

Table 4.21	Assessment of the comparison performance of penetration depth for WSCH:WNR array based on all synthetic models with electrode spacing of 1 m	94
Table 4.22	Assessment of the comparison performance of horizontal data coverage for WSCH:WNR array based on all synthetic models with electrode spacing of 1 m	94
Table 4.23	Assessment of the comparison performance of vertical data coverage for WSCH:WNR array based on all synthetic models with electrode spacing of 1 m	95
Table 4.24	Assessment of the comparison performance of sensitivity index for WSCH:WNR array based on all synthetic models with electrode spacing of 1 m	96
Table 4.25	Assessment of the comparison performance of penetration depth for PDP:WNR array based on all field study with electrode spacing of 1 m	102
Table 4.26	Assessment of the comparison performance of vertical data coverage for PDP:WNR array based on all field study with electrode spacing of 1 m	102
Table 4.27	Assessment of the comparison performance of vertical data coverage for PDP:WNR array based on all field study with electrode spacing of 1 m	103
Table 4.28	Assessment of the comparison performance of penetration depth for PDP:WSCH array based on all field study with electrode spacing of 1 m	105
Table 4.29	Assessment of the comparison performance of horizontal data coverage for PDP:WSCH array based on field study with electrode spacing of 1 m	106
Table 4.30	Assessment of the comparison performance of vertical data coverage for PDP:WSCH array based on all field study with electrode spacing of 1 m	107
Table 4.31	Assessment of the comparison performance of penetration depth for PDP:DPD array based on all field study with electrode spacing of 1 m	109
Table 4.32	Assessment of the comparison performance of horizontal data coverage for PDP:DPD array based on all field study with electrode spacing of 1 m	110

Table 4.33	Assessment of the comparison performance of vertical data coverage for PDP:DPD array based on all field study with electrode spacing of 1 m	111
Table 4.34	Assessment of the comparison performance of penetration depth for DPD:WNR array based on all field study with electrode spacing of 1 m	113
Table 4.35	Assessment of the comparison performance of horizontal data coverage for DPD:WNR array based on all field study with electrode spacing of 1 m	114
Table 4.36	Assessment of the comparison performance of vertical data coverage for DPD:WNR array based on all field study with electrode spacing of 1 m	115
Table 4.37	Assessment of the comparison performance of penetration depth for DPD:WSCH array based on all field study with electrode spacing of 1 m	117
Table 4.38	Assessment of the comparison performance of horizontal data coverage for DPD:WSCH array based on all field study with electrode spacing of 1 m	118
Table 4.39	Assessment of the comparison performance of vertical data coverage for DPD:WSCH array based on all field study with electrode spacing of 1 m	119
Table 4.40	Assessment of the comparison performance of penetration depth for WSCH:WNR array based on all field study with electrode spacing of 1 m	121
Table 4.41	Assessment of the comparison performance of horizontal data coverage for PDP:WNR array based on all field study with electrode spacing of 1 m	121
Table 4.42	Assessment of the comparison performance of vertical data coverage for PDP:WNR array based on all field study with electrode spacing of 1 m	122
Table 4.43	Summary of max penetration depth, horizontal data coverage, vertical data coverage and N level for synthetic models and field study	124
Table 4.44	Summary of assessment of the comparison performance for synthetic models and field study with electrode spacing of 1 m	124

Table 4.45	Summary of assessment of the comparison performance of sensitivity index for synthetic models with electrode spacing of 1 m	127
Table 5.1	Conclusion of assessment of the performance for penetration depth and horizontal / vertical coverage data for synthetic models with electrode spacing of 1 m	129
Table 5.2	Conclusion of assessment comparative of sensitivity index for synthetic models with electrode spacing of 1 m	130
Table 5.3	Conclusion of assessment of the performance for penetration depth and horizontal / vertical coverage data for field study with electrode spacing of 1 m	131

## LIST OF FIGURES

	<b>Page</b>
Figure 2.1 Electrode's arrangement for $\gamma 11n$ array (modified after Szalai et al., 2014a)	6
Figure 2.2 Electrode's arrangement for Midpoint null (MAN), Wenner- $\gamma$ null and Schlumberger null arrays (modified after Falco et al., 2013)	7
Figure 2.3 Electrode's arrangement for square array (modified after Lane et al., 1995)	8
Figure 2.4 Electrode's arrangement for Multiple-gradient array with a current electrode separation of $(s+2)a$ , where the separation factor $s=7$ , the $n$ factor $=2$ and the midpoint factor $m = -2$ (modified after Dahlin and Zho, 2006)	9
Figure 3.1 Basic principle of ground resistivity measurement (modified after Robinson and Coruh, 1988)	20
Figure 3.2 Electrode's arrangement for resistivity survey; a) resistivity depth sounding and b) resistivity profiling (modified after Reynolds, 1997)	21
Figure 3.3 Electrical resistivity with relation to resistance, $R$ ; area, $A$ and length, $l$ (modified after Kaerey and Brooks, 1991)	22
Figure 3.4 A conventional of resistivity measurement with four electrode arrangement (modified after Loke, 2004)	23
Figure 3.5 Basic current and potential electrodes arrangement in electrical resistivity method (modified after Telford et al., 1990)	24
Figure 3.6 Electrode's arrangement for Wenner array (modified after Loke, 2004)	27
Figure 3.7 Electrode's arrangement for Wenner-Schlumberger array (modified after Loke, 2004)	28
Figure 3.8 Comparison of electrode arrangement and cross section data pattern for Wenner and Schlumberger arrays (modified after Loke, 2004)	29

Figure 3.9	Electrode's arrangement for Dipole-dipole array (modified after Loke, 2004)	30
Figure 3.10	Electrode's arrangement for forward and reverse Pole-dipole array (modified after Loke, 2004)	31
Figure 3.11	Current flow through the Earth with different electrode spacing (modified after Burger, 1992)	32
Figure 3.12	Research flowchart	35
Figure 3.13	A synthetic model of single block embedded in homogenous medium	38
Figure 3.14	A synthetic model of two blocks embedded in homogenous medium	39
Figure 3.15	A synthetic of vertical dyke model embedded in homogenous medium	39
Figure 3.16	A synthetic of contact vertical zone model embedded in homogenous medium	40
Figure 3.17	A synthetic of fault model embedded in homogenous medium	41
Figure 3.18	Penang Island geological map (modified after Ong, 1993)	42
Figure 3.19	The survey area on the USM campus at Padang Minden. The dashed line indicates the survey line	42
Figure 4.1	Inversion result of single block model using WNR array; (a) single block model (b) datum point arrangement and (c) 2-D resistivity inversion model	45
Figure 4.2	Inversion result of single block model using WSCH array; (a) single block model (b) datum point arrangement and (c) 2-D resistivity inversion model	46
Figure 4.3	Inversion result of single block model using DPD array; (a) single block model (b) datum point arrangement and (c) 2-D resistivity inversion model	48
Figure 4.4	Inversion result of single block model using PDP array; (a) single block model (b) datum point arrangement and (c) 2-D resistivity inversion model	49
Figure 4.5	Inversion result of two block model using WNR array; (a) two block model (b) datum point arrangement and (c) 2-D resistivity inversion model	51

Figure 4.6	Inversion result of two block model using WSCH array; (a) two block model (b) datum point arrangement and (c) 2-D resistivity inversion model	52
Figure 4.7	Inversion result of two block model using DPD array; (a) two block model (b) datum point arrangement and (c) 2-D resistivity inversion model	54
Figure 4.8	Inversion result of two block model using PDP array; (a) two block model (b) datum point arrangement and (c) 2-D resistivity inversion model	55
Figure 4.9	Inversion result of contact vertical zone model using WNR array; (a) contact vertical zone model (b) datum point arrangement and (c) 2-D resistivity inversion model	57
Figure 4.10	Inversion result of contact vertical zone model using WSCH array; (a) contact zone model (b) datum point arrangement and (c) 2-D resistivity inversion model	58
Figure 4.11	Inversion result of contact vertical zone model using DPD array; (a) contact zone model (b) datum point arrangement and (c) 2-D resistivity inversion model	60
Figure 4.12	Inversion result of contact vertical zone model using PDP array; (a) contact zone model (b) datum point arrangement and (c) 2-D resistivity inversion model	61
Figure 4.13	Inversion result of vertical dyke model using WNR array; (a) vertical dyke model (b) datum point arrangement and (c) 2-D resistivity inversion model	63
Figure 4.14	Inversion result of vertical dyke model using WSCH array; (a) vertical dyke model (b) datum point arrangement and (c) 2-D resistivity inversion model	64
Figure 4.15	Inversion result of vertical dyke model using DPD array; (a) vertical dyke model (b) datum point arrangement and (c) 2-D resistivity inversion model	66
Figure 4.16	Inversion result of vertical dyke model using PDP array; (a) vertical dyke model (b) datum point arrangement and (c) 2-D resistivity inversion model	67
Figure 4.17	Inversion result of fault model using WNR array; (a) fault model (b) datum point arrangement and (c) 2-D resistivity inversion model	69

Figure 4.18	Inversion result of fault model using WSCH array; (a) fault model (b) datum point arrangement and (c) 2-D resistivity inversion model	70
Figure 4.19	Inversion result of fault model using DPD array; (a) fault model (b) datum point arrangement and (c) 2-D resistivity inversion model	71
Figure 4.20	Inversion result of fault model using PDP array; (a) fault model (b) datum point arrangement and (c) 2-D resistivity inversion model	72
Figure 4.21	Field survey results using WNR array; (a) apparent resistivity data point arrangement and (b) 2D resistivity inversion	98
Figure 4.22	Field survey results using WSCH array; (a) apparent resistivity data point arrangement and (b) 2D resistivity inversion	98
Figure 4.23	Field survey results using DPD array; (a) apparent resistivity data point arrangement and (b) 2D resistivity inversion	99
Figure 4.24	Field survey results using PDP array; (a) apparent resistivity data point arrangement and (b) 2D resistivity inversion field survey	100
Figure 4.25	Summary of assessment of the comparison performance of penetration depth for synthetic models and field study with electrode spacing of 1 m	125
Figure 4.26	Summary of assessment of the comparison performance of horizontal / vertical data coverage for synthetic models and field study with electrode spacing of 1 m	126
Figure 4.27	Summary of assessment of the comparison performance of sensitivity index for synthetic models with electrode spacing of 1 m	127



## LIST OF SYMBOLS

$\alpha$	Alpha
$\beta$	Beta
$\gamma$	Gamma
kg	Kilogram
m	Meter
m <sup>2</sup>	Meter squared
m <sup>3</sup>	Cubic meter
v	Volt
$\rho$	Resistivity
$\pi$	Pi (3.14...)
$\Omega$	Ohm
$\Omega.m$	Ohm.meter
/	Division
	Absolute value
-	Subtraction
+	Addition
*	Multiplication
%	Percent
<	Less than
>	more than

## LIST OF ABBREVIATIONS

1-D	One Dimension
2-D	Two Dimension
3-D	Three Dimension
a	Distance between two electrodes
C1	Current one
C2	Current two
CD	Compact disc
DPD	Dipole-dipole
DC	Direct current
DES	Daqinggou Ecological Station
DOI	Depth of investigation
DLA	Data level amalgamation
ERT	Electrical resistivity tomography
ERM	Electrical resistivity method
EHR	Enhancing horizontal resolution
IP	Induced polarization
IWLIU	Institute of Wind-Sand Land Improvement and Utilization
GWL	Ground water level
GPL	Gas pipeline
L	Length of conductor
MAN	Midpoint null array
N	North
P1	Potential one
P2	Potential two
PS	Parameter sensitivity
PDP	Pole-dipole
RES2DINV	Resistivity two dimension inversion
RES2DMOD	Resistivity two dimension modelling
R	Resistance
SAS	Statistical Averaging System
SI	Sensitivity index
SP	Self potential
TCM	Topography correction method
USM	Universiti sains Malaysia
VES	Vertical electrical sounding
WNR	Wenner
WSCH	Wenner Schlumberger
Ze	Median depth of investigation

# **PENILAIAN KEUPAYAAN BAGI SUSUNATUR UMUM KEBERINTANGAN**

## **2-D**

### **ABSTRAK**

Penilaian keupayaan bagi susunatur keberintangan elektrik dilakukan untuk perbandingan kedalaman penembusan, liputan data mendatar / menegak dan indeks kepekaan bagi setiap susunatur. Tujuan kajian ini ialah untuk mengenal pasti keupayaan susunatur umum; Wenner (WNR), Wenner-Schlumberger (WSCH), Dipole-dipole (DPD), dan Pole-dipole (PDP) relatif kepada satu sama lain (PDP: WNR, PDP: WSCH, PDP: DPD, DPD: WNR, DPD: WSCH dan WNR: WSCH) dan dibentangkan dalam bentuk rangka. Lima model sintetik dan satu kajian lapangan telah diwujudkan untuk penilaian keupayaan dengan empat susunatur berlainan. Berdasarkan kepada penilaian, perbandingan bagi susunatur PDP:WNR menunjukkan perbezaan peratusan tertinggi untuk penilaian kedalaman penembusan iaitu 54.60 % bagi model sintetik dan 55.03 % bagi kajian lapangan, manakala peratusan tertinggi untuk penilaian liputan data mendatar / menegak adalah 66.67 % bagi model sintetik dan 79.88 % bagi kajian lapangan. Susunatur WSCH:WNR menunjukkan perbezaan peratusan yang rendah untuk penilaian kedalaman penembusan iaitu 10.12 % bagi model sintetik dan 10.36 % bagi kajian lapangan. Disamping itu, susunatur PDP:DPD menyampaikan perbezaan peratusan yang rendah untuk penilaian liputan data mendatar / menegak dengan nilai 5 % bagi model sintetik dan 19.04 % bagi kajian lapangan. Penilaian terakhir ialah perbandingan berangka bagi indeks kepekaan yang hanya dilaksanakan pada model sintetik. Keputusan mendedahkan bahawa perbandingan bagi susunatur PDP:DPD mempunyai perbezaan peratusan tertinggi untuk nilai kepekaan 98.20 % pada

peringkat 1 manakala peringkat 2 hingga 7 menunjukkan susunatur PDP:WSCH mempunyai perbezaan peratusan tertinggi untuk nilai kepekaan masing-masing; 91.15 %, 86.45 %, 82.86 %, 80.92 %, 79.04 %, dan 77.62 %. Perbezaan peratusan yang rendah untuk indek kepekaan menunjukkan bahawa susunatur WNR:WSCH memiliki indek kepekaan yang sama pada peringkat 1. Perbezaan peratusan yang rendah pada peringkat 2 hingga 4 iaitu susunatur PDP:DPD dengan nilai masing-masing 9.38 %, 31.35 %, dan 37.12 %. Pada peringkat 5 dan 6, Perbezaan peratusan yang rendah adalah 2.05 % (n=5) dan 39.86 % (n=6) dihasilkan oleh susunatur DPD:WNR. Perbandingan susunatur PDP:WNR mendominasi peratusan yang rendah pada peringkat n=7 hingga n=10 dengan nilai masing-masing 27.67%, 17.70%, 5.12% dan 7.53%. Sebagai kesimpulan, susunatur PDP dibentangkan sebagai susunatur terbaik berbanding dengan susunatur umum lainnya berdasarkan perbezaan peratusan pada kedalaman penembusan (33-55%), liputan data mendatar, liputan data menegak (5-80%) dan indeks kepekaan (5-98 %).

# **ASSESSMENT OF THE PERFORMANCE OF COMMON 2-D RESISTIVITY ARRAYS**

## **ABSTRACT**

The assessment of the performance for electrical resistivity arrays were carried out by comparing the penetration depth, horizontal / vertical coverage and sensitivity index of each array. The research objective is to identify the performance of common arrays; Wenner (WNR), Wenner-Schlumberger (WSCH), Dipole-dipole (DPD), and Pole-dipole (PDP) relative to each other (PDP:WNR, PDP:WSCH, PDP:DPD, DPD:WNR, DPD:WSCH and WNR:WSCH) and presented in numerical form. Five synthetic models and one field study were created for assessment of the performance using the four different arrays. Based on the assessment, the comparison of PDP:WNR array shows highest percentage difference in penetration depth for both synthetic model and field study with value of 54.60 % and 55.03 % respectively while the highest percentage difference in horizontal / vertical coverage is 66.67 % for synthetic model and 79.88 % for field study. The WSCH:WNR array shows lowest percentage difference for penetration depth with value of 10.12 % for synthetic model and 10.36 % for field study. On the other hand, the PDP:DPD array shows lowest percentage difference of assessment for horizontal / vertical coverage with value of 5 % for synthetic model and 19.04 % for field study. The last assessment was sensitivity index which was only applied to the synthetic model. The comparison of PDP:DPD array shows the highest percentage difference of sensitivity index of 98.20 % at level 1 while at level 2 to 7, PDP:WSCH array showed highest percentage difference of 91.15 %, 86.45 %, 82.86 %, 80.92 %, 79.04 %, and 77.62

% respectively. The lowest percentage different of sensitivity index shows that the WNR:WSCH array has the identical sensitivity index with no different observed at level 1. The lowest percentage for level 2 to 4 is PDP:DPD array with value of 9.38 %, 31.35 % and 37.12 % respectively. For level 5 and 6, the lowest percentage difference are 2.05 % (n=5) and 39.86 % (n=6) produced by DPD:WNR array. PDP:WNR array comparison dominated the lowest percentage at n=7 to n=10 with values of 27.67 %, 17.70 %, 5.12 % and 7.53 % respectively. As a conclusion, PDP array presented as the best array compare with another common array based on percentage difference of penetration depth ( 33-55 %), horizontal data coverage, vertical data coverage (5-80 %) and sensitivity index (5-98 %).

# CHAPTER 1

## INTRODUCTION

### 1.0 Background

For decades, resistivity has been one of the most popular investigation method in geophysics which is applied in hydrogeology, subsurface exploration, mining, geotechnical and archaeological works. Resistivity method has been developing rapidly for geophysics investigation and became the main technology for several researches in assisting geoscientists to further understand the features of the Earth's subsurface. The popularity of the method is due to the short period of time required for collection and processing of the data. In resistivity investigation, a suitable array of electrode arrangement is applied depending on the objective of the study. Each array has its own advantages / disadvantages and limitations regarding field operations, interpretation capabilities, sensitivity index to horizontal / vertical variations, signal strength and depth of investigations (Ishola et al., 2015).

Many researchers have conducted resistivity investigations regarding the results of various arrays. Several arrays commonly used in applied geophysical investigations include Wenner, Schlumberger, Dipole-dipole and Pole-dipole. The performance of each array are not documented and not much in-depth studies were done regarding the arrays themselves. This research was conducted to study the performance of the common arrays in terms of depth of investigation (DOI), sensitivity index, horizontal data coverage and vertical data coverage. Comparisons between the arrays were discussed in this study and tabulated for future reference.

## **1.1 Problem statements**

Electrode array is one of the important factors for ground resistivity investigation in order to optimize data quality and achieve objectives of the study. According to Loke (2016), Wenner array provides good vertical resolution in noisy area with limited survey time, while Dipole-dipole is suitable in providing good horizontal resolution with good data coverage. On the other hand, Pole-dipole array produces good penetration depth with limited number of electrodes and Schlumberger array provides good horizontal and vertical resolutions. At present, the comparison assessment did not present any numerical form statements that clearly explain the percentage difference of the common arrays. This study was conducted to determine and tabulate the performance difference between the common arrays and possibly identify more advantages / disadvantages of the arrays.

## **1.2 Research objectives**

The objectives of this research are:

- i. To compare assessment of the performance of common arrays (Wenner, Wenner-Schlumberger, Dipole-dipole and Pole-dipole).
- ii. To produce performance (penetration depth, vertical data coverage, horizontal data coverage and sensitivity index) tables for Wenner, Wenner-Schlumberger, Dipole-dipole and Pole-dipole arrays.
- iii. To determine the best array based on assessment of the performance.



### **1.3 Scope of study**

This study assess the performance of common array (Wenner, Wenner-Schlumberger, Dipole-dipole and Pole-dipole arrays) refer to penetration depth, horizontal data coverage, vertical data coverage and sensitivity index without considering the resistivity value ( $\rho_a$  or  $\rho_t$ ). The synthetic models were design base on five common geology condition / setting which is provided by Res2Dmod software using resistivity value of 100  $\Omega$ .m, 200  $\Omega$ .m and 700  $\Omega$ .m and minimum electrode spacing of 1 m. The field study was carried out at Universiti Sains Malaysia, Pulau Pinang (Malaysia) using 1 m minimum electrode spacing. The data was collected using ABEM SAS4000 system and process using Res2Dinv, Res2Dmod, Microsoft Office Excel, and Surfer 8.

### **1.4 Significant and novelty**

Previous studies have not explained clearly concerning assessment performance of arrays used. The researchers only provided a statement that Pole-dipole array is relatively good for horizontal coverage and produces higher signal strength compared to Dipole-dipole array. However, the Dipole-dipole array has better horizontal data coverage than Wenner array. The penetration depth of array depends on current electrode spacing and from the previous study. Wenner array produced shallower depth compared to Dipole-dipole (Okpoli, 2013 and Loke, 2004). This study demonstrates the assessment performance between common arrays (Wenner, Wenner-Schlumberger, Dipole-dipole and Pole-dipole) by assessing the aspect of each array and finally producing a performance table.

## **1.5 Thesis layout**

This thesis consists of five chapters. The first chapter is introduction which includes research introduction, problem statements, research objectives, scope of study, significance and novelty. Chapter Two is the literature review which consists of several studies conducted by other researchers using resistivity method applied in environmental and engineering fields with Wenner, Wenner-Schlumberger, Dipole-dipole and Pole-dipole arrays as their choice of electrode arrangements. The third chapter discusses the methodology throughout this study which consists of the basics in electrical resistivity method and its principles. Chapter Four provides a discussion of results obtained from this study and it also expresses the significant information about the study which are performance and numerical form. Finally, Chapter Five is the conclusion of this research including some recommendations which can be applied for the future research.

## CHAPTER 2

### LITERATURE REVIEW

#### 2.0 Introduction

With the development of research and science, resistivity method has not been considered as a traditional method since 2-D and 3-D resistivity have been introduced (Loke, 2016). Generally, the resistivity survey are done to predict ground subsurface resistivity distribution of the Earth using selected electrode array (Wenner, Schlumberger, Dipole-dipole and Pole-dipole). Each array has their own advantage / disadvantage and the selection of a specific array depends on the objective of the study and that particular array may not be suitable for another objective. Using resistivity survey with selected array, four characteristics need to be considered, namely depth of investigation (DOI), sensitivity index, signal strength, horizontal data converge and vertical data converge. Previous works presented knowledge about the real acquisition and computer modeling, using some resistivity arrays for depth of investigation, array sensitivities and suitability.

#### 2.1 Previous works

Szalai et al. (2014a) introduced a new array type which is called  $\gamma 11n$  array (Figure 2.1). The array produced good investigation result in horizontal and vertical resolution including shorter measuring time. Based on numerical studies, the array was able to identify the characteristics of tunnels, caves, cables and buried tubes in

clay layer and it also showed increment in terms of the effectiveness of electrical resistivity tomography.

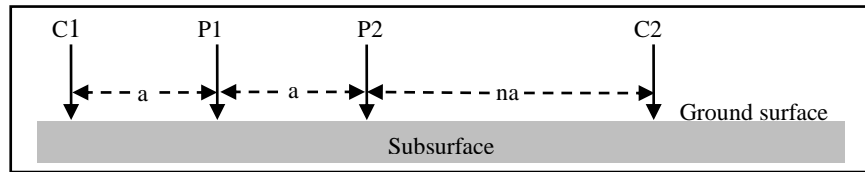


Figure 2.1: Electrode's arrangement for  $\gamma 11n$  array (modified after Szalai et al., 2014a).

Depth of investigation is one of the crucial parameters in geophysical exploration. Szalai et al. (2014b) discussed the depth of investigation (DOI) for 2-D electrical resistivity tomography using  $\gamma 11n$  array and provided solution about depth of investigation. The research explained a relation between maximum values of parameter sensitivity (PS) maps with DOI value. The array measured has higher PS value than other classical arrays. As a conclusion, The  $\gamma 11n$  require moreover less measurement than most conventional arrays resulting in shorter measuring time.

A research in an urban environment, such a noisy area and limited measuring area (restricted), was conducted by Szalai et al. (2011) to investigate the depth of investigation. The study used six different resistivity arrays (Wenner- $\alpha$ , Wenner- $\beta$ , Pole-pole, Dipole- equatorial, Pole-dipole, and Dipole-axial) including several noise levels. The results showed that Pole-dipole (PDP) and Dipole-axial (DP-axial) arrays should be recommended as default selections since these arrays provided the best depth of investigation.

Falco et al. (2013) studied the behavior of three Null-arrays (Figure 2.2); Midpoint null array (MAN), Wenner- $\gamma$  null array and Schlumberger null array in response to fracture characterization in Les Breuleux (Switzerland). The purpose of the study was to determine which array is the best in locating fractures. The results showed that the most accurately for localise vertical fractures is Wenner- $\gamma$  and Schlumberger null-arrays, while the midpoint null-array and Schlumberger null-array allows accurate orientation of a fracture. However, based on the numerical result, the Midpoint-null array was specifically efficient in the fractures orientation study. As a conclusion, the resistivity null-array was more suitable than the classical array for identification of fractures geometry characteristic.

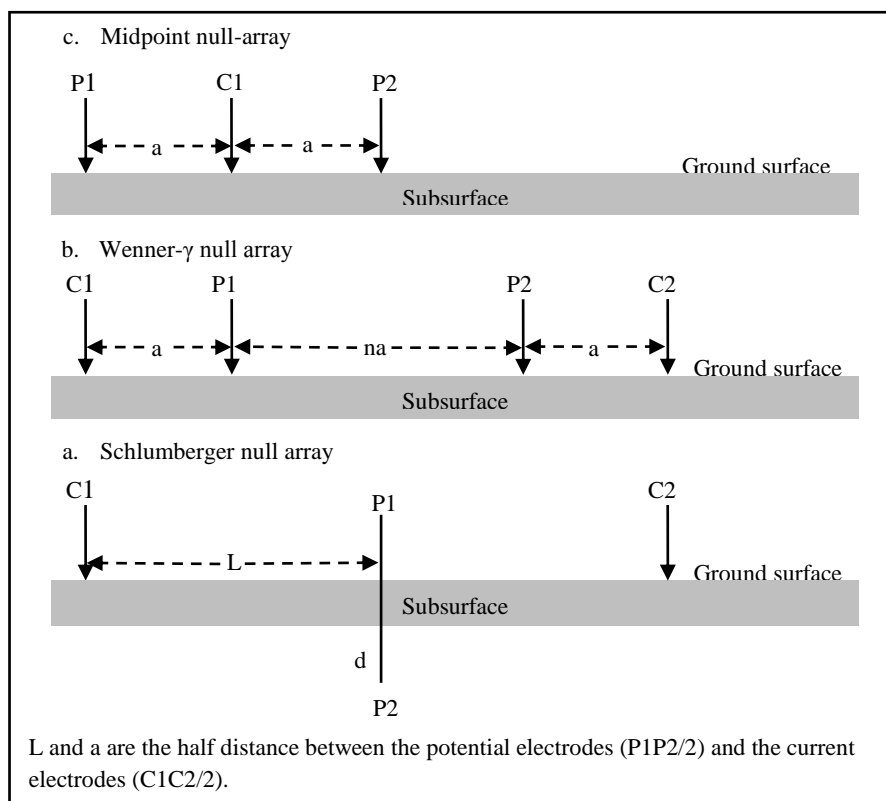


Figure 2.2: Electrode's arrangement for Midpoint null (MAN), Wenner- $\gamma$  null and Schlumberger null arrays (modified after Falco et al., 2013).

Ishola et al. (2015) have been investigated the electrical resistivity capabilities using *k*-mean clustering. *k*-mean known as an the unsupervised classification technique. The assessment of the performance was carried out using an error matrix, mean absolute error and mean absolute percent error. The result showed that *k*-mean presented good agreement between true block models and combined classified imaged. The overall shows the accuracy range of 86-99 % while K-mean coeficience is 54-98 %.

Lane et al. (1995) applied direct-current (DC) for resistivity sounding method using square array (Figure 2.3) to detect fractures in Grafton County, New Hampshire. The study also supported by another geophysical method such as seismic refraction and DC 2-D resistivity with Schlumberger array. As a conclusion, DC 2-D resistivity sounding with square array was more sensitive to explain rock anisotropy compare to traditional array (Schlumberger and Wenner).

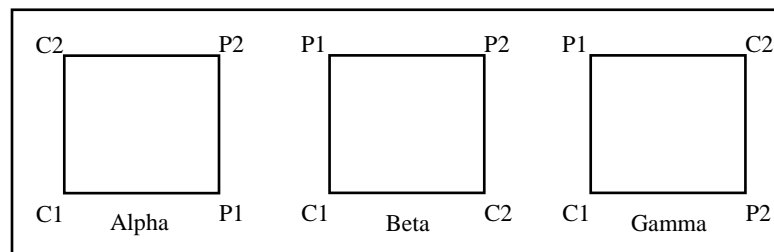


Figure 2.3: Electrode's arrangement for square array (modified after Lane et al., 1995).

Dahlin and Zho (2006) used Multiple-gradient (Figure 2.4), Wenner and Dipole-dipole arrays for data acquisition in Sweden and Nicaragua. The study was done to confirm the practical applicability result with numerical modeling. The result showed that the Multiple-gradient array with multiple current electrode combinations provided a good resolution compared to Wenner array. The Multiple-gradient array

was more suitable for multichannel data acquisition since it can provide higher data density and a time-saver in data acquisition. The Wenner array was not suitable for measuring using the multichannel system because it provided lowest sensitivity to noise ratio among the arrays studied.

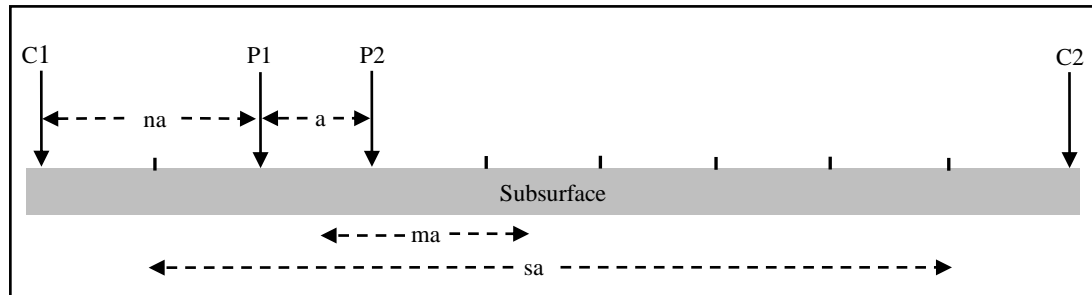


Figure 2.4: Electrode's arrangement for Multiple-gradient array with a current electrode separation of  $(s+2)a$ , where the separation factor  $s=7$ , the  $n$  factor  $=2$  and the midpoint factor  $m = -2$  (modified after Dahlin and Zho, 2006).

Okpoli (2013) used several arrays (Pole-pole, Pole-dipole, Pole-bipole, Dipole-dipole, Wenner, Wenner- $\beta$ , Wenner- $\gamma$ , Gradient, Midpoint-potential-referred, Schlumberger, Square and Lee-partition) to study the sensitivity and resolution capacity. The study showed that the Gradient array gave good spatial resolution, while Midpoint-potential-referred array was the most suitable for multichannel measurement in the field due to its lower noise sensitivity and also lower spatial resolution of the image.

Bery (2014) used 2-D sensitivity computerized modeling method to analyse depth of investigation factors ( $Z_m/a$  and  $Z_m/L$ ) for Dipole-dipole, Pole-dipole and Wenner-Schlumberger arrays. The study provided great enhancements in field measurement including cost reduction and high resolution. The researcher introduced a new hybrid array called Andy-Bery array that was successful and reliable in imaging conductive model resistivity with actual dimension.

Al Moush and Mashagbeh (2009) conducted a case study on geotechnical application in Jordan using geophysical methods to image near-surface cylindrical pipeline. The survey applied magnetic method to study anomaly response and electrical resistivity imaging using Wenner array to investigate an underground gas pipeline (GPL). The geomagnetic survey revealed the GPL in the form of dimension and extension. The electrical resistivity imaging was effective in mapping the subsurface lithology including shallow structure fractures. The study was successful in imaging the underground GPL for different soil materials with depths of 1-4 m.

Generally, the resistivity survey using common conventional arrays, such as Wenner, Schlumberger, Dipole-dipole, Pole-dipole and Pole-pole arrays, is ineffective because of cost and time consumption. Aizebeokhai and Oyeyemi. (2014) applied Multiple-gradient array, a non-conventional array, to conduct 2-D resistivity and time domain induced polarization (IP) at Ota, southwestern Nigeria. The research applied inverse resistivity and chargeability to obtain subsurface characteristic of the study area. The results showed that Multi-gradient array is good for that particular case because it was fast in data acquisition, cost effective, a suitable array for conducting 2-D resistivity and IP surveys, and it also improved image resolution.

Song et al. (2012) conducted a study by comparing the estimation of ground water level (GWL) using Wenner array, for vertical electrical sounding (VES), with manually monitoring wells. The study area consists of two locations which are Daqinggou Ecological Station (DES) and Institute of Wind-Sand Land Improvement and Utilization (IWLIU) which is a semi arid area located in South Keerqin sandy aquifer, China. The result showed that GWL variation between VES method and



manual measurement ranged of 0.22-1.03 m at DES and 0.03-0.82 m at IWLIU. In conclusion, VES method was a good measuring tool for estimating GWLs in unconfined sandy aquifers while GWL is sufficiently deep of more 3.98 m.

Vega et al. (2003) studied a combination of inversion model for Wenner and Dipole-dipole arrays for contamination of soil due to gasoline spill. The study showed that the combination of Wenner and Dipole-dipole arrays improved penetration depth to 25 m which referred to the actual depth of Dipole-dipole and Wenner arrays which are 20 m and 16 m respectively.

Alwan (2013) used 2-D electrical resistivity imaging techniques with Wenner, Dipole-dipole and Wenner-Schlumberger arrays to identify shallow subsurface structure in University of Technology Camp, Bagdad, Iraq. The study's aim was to identify the best classical array suitable for case study which consists of silty clay, clay and sand. Borehole data was used to confirm the resistivity value and a total of six 2-D images were created where two of the images were assigned for each array. The length of each image is 60 m with depth of 8-12 m. The results concluded that the Wenner-Schlumberger array provided the best array for the study area since it gave deeper penetration than the other arrays (Dipole-dipole array by 8.27 m, Wenner-Schlumberger array by 12.1 m and Wenner array by 10.2 m).

Martinez-Lopez et al. (2013) applied Wenner-Schlumberger, Wenner and Dipole-dipole arrays with different inter-electrode spacing to detect subsurface cavities in different geological condition (granite, phyllite and sandstone). There were several factors influencing the data for subsurface cavity detection such as depth, diameter of the cavity, array use, electrode spacing, geological setting and density of the data. The result showed that Wenner-Schlumberger array provided

good resolution capacity in three cases studied of cavities excavated in a variety of different lithologies when compared to Wenner and Dipole-dipole arrays in detecting cavities.

Metwaly and Alfouzan (2013) used 2-D resistivity tomography in detecting subsurface cavity for civil engineering and environmental management in eastern part of Saudi Arabia. Generally, geomorphology of the area was karstic, limestone with sinkholes. The study was conducted using Wenner-Schlumberger array with seven 2-D electrical resistivity profiles in the new urbanization of Al Hassan area. The data processing was simulated with physical model based on common karstic features of the area. The results showed that the inverted resistivity data represents the resistivity distribution to maximum depth of about 15 m and the shallow weathered zone consists of two important features; subsurface cavities and subsurface weathered zones with low resistivity values of  $<24 \Omega.m$ .

The geometry and dimension of space are two of the important factors in geotechnical, archeological, speleological studies, and quarrying activities. Study conducted by Abu-Shariah (2009) used minimum electrode spacing of 2 m to make a total spread length of 98 m, applied 2-D resistivity imaging method using Wenner- $\alpha$  array to determining shape and size of a cave. The resulting inverse model presented the location and extent of a subterranean with low resistivity anomaly ( $<115 \Omega.m$ ) which was interpreted as a cavity.

Szokoli et al. (2013) presented Wenner  $\gamma$ 11n array as a new electrical resistivity tomography (ERT) array to increase the depth of detectability. The study used a prism and dyke models to investigate the case. The result showed that the Wenner  $\gamma$ 11n array provided a systematically (consistently) higher depth of

detectability value than Pole-dipole and Dipole-axial array, and more information was gained in less acquisition time.

Bery (2016) applied two different optimized arrays (Wenner-Schlumberger and Pole-dipole) to present development of the data level amalgamation (DLA) technique in resistivity data processing for groundwater exploration. The research was conducted in Taiping, Perak (Malaysia) with the study line having a total length of 400 m for Wenner-Schlumberger array and 800 m for Pole-dipole array using minimum electrode spacing of 10 m for each array. Both of the arrays shared the same center for the resistivity line. The results showed that the DLA technique was capable in enhancing horizontal model resistivity resolution with added topography and increasing the penetration depth up to 335 m.

Neyamadpour et al. (2010) studied the comparison between Dipole-dipole and Wenner arrays in delineating an underground cavity. The study was designed in gridding path and carried out along seven parallel survey lines. The electrode spacing chosen were different for each array, whereby for the Wenner array five different electrode spacings were assembled ( 1, 2, 3, 4 and 5 times of minimum electrode spacing) while for the Dipole-dipole array three different electrode spacings were used (1, 2, and 3 times of minimum electrode spacing). The results showed that the Wenner array was better than the Dipole-dipole array in determining the vertical distribution of the subsurface resistivity. While the Dipole-dipole array presented a better lateral extent of the subsurface features.

Bery et al. (2014) optimized Wenner-Schlumberger and Pole-dipole arrays to present high resolution time-lapse resistivity tomography study for slope monitoring at Minden, Penang Island (Malaysia). The length of the study line was 40 m with 1 m

minimum electrode spacing. The inversion result suggested that the optimization were effective as the merging of the two arrays provided high resolution data. The results provided a total of 2052 datum points and satisfactory horizontal and vertical resolution were obtained including an increased penetration depth of up to 15.10 m. These are increments of 6 % of penetration depth for Pole-dipole and 51 % for Wenner-Schlumberger.

Muztaza et al. (2013a) applied enhancing horizontal resolution (EHR) technique using Pole-dipole array at three study areas in Malaysia; Pagoh and Nusajaya (Johor), and Puchong (Selangor). The HER technique is the improved technique in improving the vertical resolution. The objective of the study was to map and characterize shallow subsurfaces of each study area. In Pagoh (Johor), the 2-D resistivity and induced polarization were used to detect the subsurface variations of resistivity and chargeability of iron ore. The results showed a bedrock underlain by a thick alluvium with resistivity value between 10-800  $\Omega$ .m and chargeability rate of 0.1-3 ms. A sedimentary area, which is Nusajaya (Johor) showed resistivity value for sandstone containing iron ore mineral ranging from 30-250  $\Omega$ .m and weathered sandstone was 500-1000  $\Omega$ .m. In Puchong (Selangor), the 2-D resistivity result showed a low resistivity value of <40  $\Omega$ .m. As a conclusion, a stratigraphy and structure of the three case studies was mapped effectively using 2-D resistivity with EHR with improved good horizontal and vertical resolution.

Muztaza et al. (2013b) used Pole-dipole array with enhancing horizontal resolution (EHR) technique to determine the thickness of alluvium in Lembah Bujang (Kedah). The survey was carried out with 1 m minimum electrode spacing. The results showed that the research area consists of alluvium with resistivity value

of 0-500  $\Omega$ .m and the alluvium was classified into two layers; top layer consists of clay with resistivity value 0-5  $\Omega$ .m and second layer is sandy clay/sand with resistivity value of 8-300  $\Omega$ .m. In the research, the EHR technique had improved the horizontal resolution in the subsurface resistivity for area study.

Saufia et al. (2012) applied the combination of 2-D electrical imaging with Pole-dipole array and self potential (SP) method to investigate the presence of saturated zones due to engineering problems. There were six survey lines (four lines for resistivity and two lines for SP) with 4 m spacing stations (porous pot). The results showed that the subsurface consists of a saturated zone with a resistivity value of <30  $\Omega$ .m at depth of 5 to 20 m, meanwhile SP result showed water flow in different directions.

Saad et al. (2017) studied the origin of sediment deposition of Sungai Batu, which is an ancient river area. The study used two geophysical methods; 2-D resistivity using Pole-dipole array with 2.5 m electrode spacing and seismic refraction tomography with 5 m geophone spacing using 5 kg sledgehammer as the seismic source. There are 3 major soil types found in the study area. The first layer was top soil with resistivity value of >100  $\Omega$ .m which was interpreted as loose and dry alluvium. The second was saturated alluvium with resistivity value of 10-50  $\Omega$ .m and velocity value of <1400 m/s which was interpreted as clay and sand. The third layer was moist with resistivity value of <100  $\Omega$ .m. In addition, the resistivity value of >300  $\Omega$ .m and velocity value of >3600 m/s was identified as the river bed of the study area. In conclusion, the depositional environment in this research was due to land sediment deposit.

Saad et al. (2014) did a research on archaeology anomaly in Sungai Batu, Lembah Bujang, Kedah (Malaysia) using 2-D resistivity profiles. The research applied Pole-dipole array with a total of 15 lines with 0.75 m minimum electrode spacing and 2 m line spacing. The study area was designed in a grid path. The study concluded that the study area consists of alluvium with resistivity value of  $>50 \Omega.m$  and the anomaly identified was at depth between 0-1 m with resistivity value of  $>3500 \Omega.m$  and it was interpreted as baked clay bricks.

A subsurface study was conducted by Saad et al. (2011) using 2-D resistivity method using Pole-dipole array with 5 m minimum electrode spacing. The purpose of the study was to identify meteorite impact in Bukit Bunuh, Perak. The total length of the survey line of the area was 8 km and parallel to Sungai Perak, Bintang Range and Titiwangsa Range. The result showed resistivity value of 10-800  $\Omega.m$  and thickness from 5-60 m for the first zone which was indicated as alluvium consisting boulder with resistivity value of  $>6000 \Omega.m$ . While resistivity value of  $>2000 \Omega.m$  was indicated as bedrock which was interpreted as the second zone.

Saad et al. (2013) estimated an overburden and rock volume at Masai quarry, Johor Darul Takzim. The study applied 2-D resistivity imaging method with Pole-dipole array. There were six survey lines used in the study area with 5 m minimum electrode spacing. The results showed that the research area consists of two main zones, where the first zone was residual soil with resistivity value of  $<700 \Omega.m$ . This zone was interpreted as saturated zone with resistivity value of 30-100  $\Omega.m$  and boulder with resistivity value of  $>700 \Omega.m$ . In addition, fractured granitic bedrock was considered as the second zone which had resistivity value of  $>1000 \Omega.m$  and

depth of 10-75 m. Lastly, the overburden of study area consists of residual soil was mixed with boulders with overburden volume is around  $9 \text{ m}^3$ ,  $811 \text{ m}^3$  and  $831.15 \text{ m}^3$ .

Saad et al. (2012) used 2-D electrical resistivity tomography for groundwater detection in alluvium soil areas. The survey lines were conducted in two different areas. The first area was in Selangor with a total length of survey line at 200 m and the second area was in Pahang which consists of three survey lines (two lines with a total length of 400 m in Pematang Lawang and one line with a total length of 300 m in Inderapura). The research used Pole-dipole array with 5 m electrode spacing. Overall, the results showed that the study area consists of alluvium overburden with resistivity value of  $<800 \text{ } \Omega \cdot \text{m}$ . In addition, the groundwater reservoirs were found in saturated sand, saturated sandy clay and saturated silt, clay and sand.

A study to locate buried furnace in Sik, Kedah was conducted by Muztaza et al. (2014) using 2-D resistivity imaging method with Pole-dipole array and it was designed in gridding model. The survey line was divided into two groups. The first group consists of 11 survey lines with 0.5 m minimum electrode spacing and 1 m interval line spacing. The second group consists of 4 survey lines with 0.5 m minimum electrode spacing and 1.5 m interval line spacing. The result showed resistivity value of  $<15 \text{ } \Omega \cdot \text{m}$  at depth between 0-1.5 m which was regarded as buried furnace.

## **2.2 Summary**

Application of resistivity method in studying resistivity values has developed extensively in various fields such as geophysics, archeology, engineering, and

hydrology. The common arrays used in studying characteristics of the subsurface within an area were Wenner, Schlumberger, Dipole-dipole and Pole-dipole. Several researchs have been carried out regarding the performance and efficiency of several electrode arrays configuration (Muztaza et al., 2014; Saad et al., 2013; Szalai et al., 2014a; Okpoli, 2013; Ishola et at., 2015). However, the studies previously reviewed did not specifically explain the application and comparison with other arrays in the sense of penetration depth, sensitivities and array suitability. The studies only discussed the depth of investigation (DOI). Furthermore, there were no numerical comparison between the common arrays used such as Wenner, Schlumberger, Dipole-dipole and Pole-dipole arrays in terms of penetration depth, sensitivity index, horizontal data coverage and vertical data coverage.



## **CHAPTER 3**

### **METHODOLOGY**

#### **3.0 Introduction**

Generally, geophysical method has greatly contributed to research and knowledge about Earth sciences especially its subsurface. Method such as electrical resistivity can be used to identify the depth of bedrock and soil material (Bery, 2015). The method provides effective answers to hydrogeology, subsurface exploration, mining, geotechnical and archaeological problems. Since the Schlumberger brothers successfully introduced the resistivity method in 1920's, the application of the method has been developing continuously until the present day (Maganti, 2008). Many of the Earth's phenomena were solved by the application of the resistivity method, especially in the investigation of the subsurface. Electrical resistivity studies were rapidly developed to study the electrical properties of rocks, soil and materials of Earth subsurface. However, in the modern era, measurements of resistivity using the method should provide shorter data acquisition time, better resolution and improved penetration depth.

#### **3.1 Electrical resistivity method**

Electrical resistivity method (ERM) has become one of the most common geophysical method used in electrical investigation. ERM has the ability to present results in image form of the Earth's subsurface effectively, efficiently and with

automated data acquisition. During data acquisition, electrodes were planted so that they are in contact with soil / rock to allow current flow within the Earth between a pair of electrodes (C1 and C2). Meanwhile, potential difference across another pair of electrodes (P1 and P2) is measured for resistivity calculation (Figure 3.1).

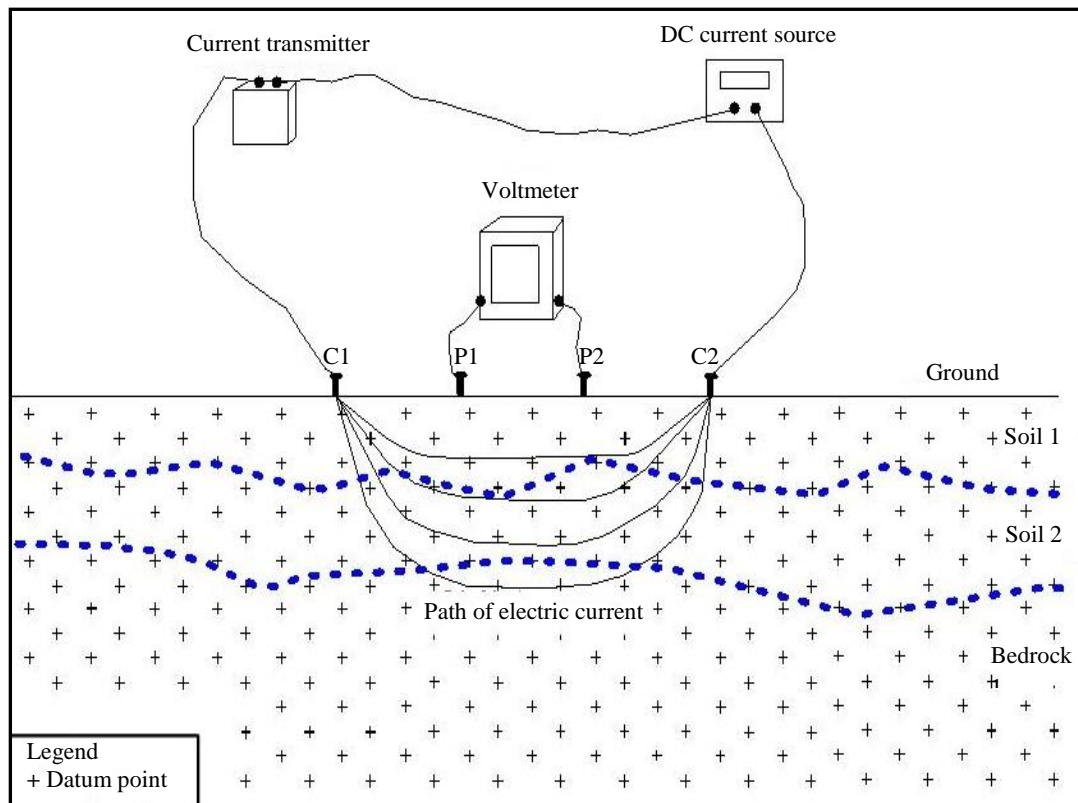


Figure 3.1: Basic principle of ground resistivity measurement (modified after Robinson and Coruh., 1988).

Theoretically, electrical resistivity is applied to measure potential difference of Earth's subsurface structure and material which opposes the current flow (Burger et al., 2006). Resistance is a ratio between the potential difference and current which depends on the material's electrical properties, size and diameter. An overall resistivity is the combination of multiple resistivity values from all layers and a body affecting the paths which is called apparent resistivity,  $\rho_a$  (Valenta, 2015).

The electrical resistivity technology had evolved significantly both in the terms of softwares and hardwares. Generally, there are two fundamental modes of resistivity survey namely; resistivity profiling and resistivity depth sounding. The resistivity depth sounding is presented to investigate the Earth's subsurface boundary. In this mode, the measurement is taken at one place with increasing separation of the current electrodes to measure different penetration depths and vertical profiles of the subsurface. On the other hand, resistivity profiling mode retains the same inter-electrode distance during the entirety of data acquisition (Figure 3.2).

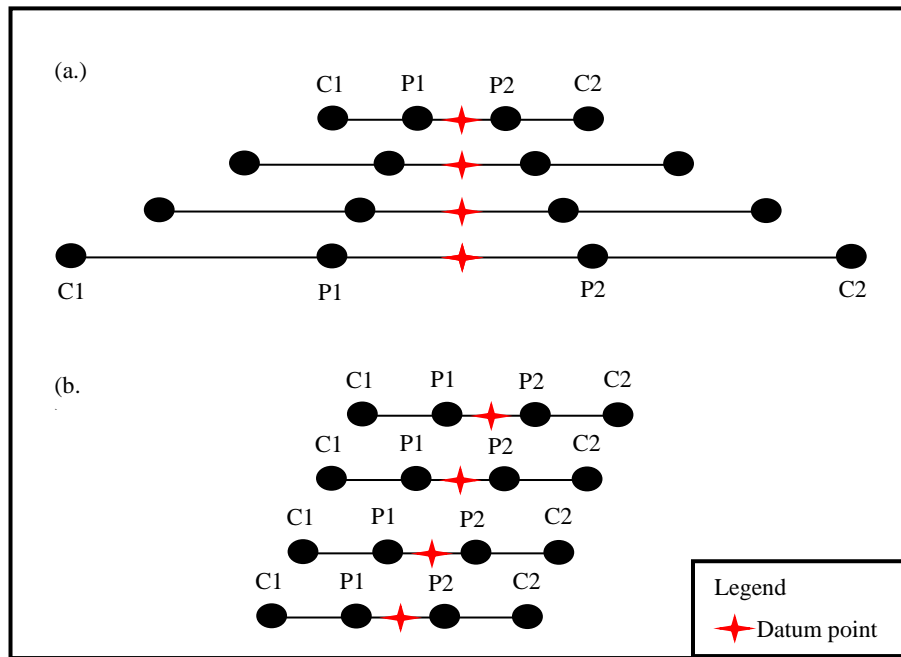


Figure 3.2: Electrode's arrangement for resistivity survey; a) resistivity depth sounding and b) resistivity profiling (modified after Reynolds, 1997).

### 3.2 Electrical resistivity

The aim of electrical resistivity work is to determine ground subsurface resistivity distribution from ground surface measurement (Loke, 2016). The electrical

current is a flow of electrically charged particles (electrons). The flow of electrical current in rock / soil follows three types of conduction procedures; electrolytic, electronic and dielectric conduction (Reynolds, 1997). Classically, current is considered flowing from positive to negative electron. Georg Simon Ohm, a German physicist, presented states of current which is directly proportional to voltage,  $V$  and inversely proportional to resistance,  $R$  (Burger, 1992). This relation is called the Ohm's Law (Equation 3.1).

$$I = \frac{V}{R} \quad (3.1)$$

where;

- $I$  = Current (Ampere, A)
- $V$  = Voltage (Volt, V)
- $R$  = Resistance (Ohm,  $\Omega$ )

Naturally, the Earth's subsurface consists of geologic materials such as soil and bedrock in which contain electrically charged particles (electrons). The resistance value is different when the current flows into the ground because of the various geologic materials. The overall resistance of a material depends on its ability to conduct current and its diameter. Theoretically, resistivity of a material is defined as the resistance between the opposite faces of a unit cube of the material. Figure 3.3 shows a cylinder with resistance,  $R$  while resistivity depends on the length and cross sectional materials, given by Equation 3.2 (Kaerey and Brooks, 1991).

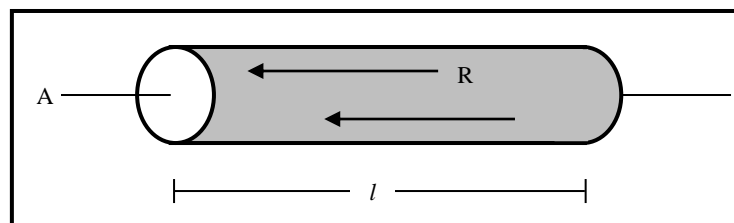


Figure 3.3: Electrical resistivity with relation to resistance,  $R$ ; area,  $A$  and length,  $l$  (modified after Kaerey and Brooks, 1991).

$$R = \rho \frac{l}{A} \quad (3.2)$$

Resistivity is written as Equation 3.3 by rearranging the Equation 3.2.

$$\rho = \frac{RA}{l} \quad (3.3)$$

where:

$\rho$  = Resistivity of the conductor material ( $\Omega.m$ )

R = Resistance

A = Cross-sectional area ( $m^2$ )

l = Length of the conductor (m)

Figure 3.4 shows an electrode arrangement used to measure ground subsurface resistivity distribution. Two current electrodes (C1 and C2) are planted into the ground to allow current flow and another pair of electrodes (P1 and P2), are potential electrodes used to measure potential different value (Loke, 2004). Equation 3.4 is used in calculating apparent resistivity,  $\rho_a$ .

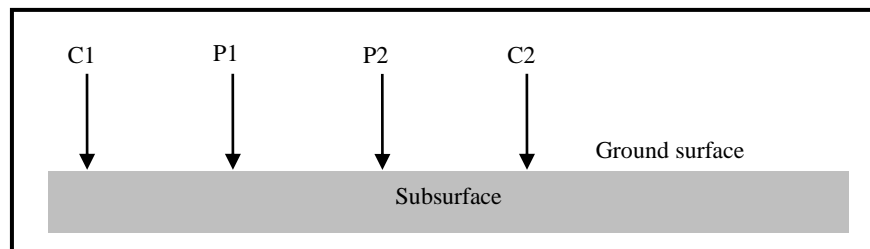


Figure 3.4: A conventional of resistivity measurement with four electrode arrangement (modified after Loke, 2004)

$$\rho_a = k \frac{V}{I} \quad (3.4)$$

where:

$\rho_a$  = Apparent resistivity ( $\Omega.m$ )

V = Voltage (volt)

k = Geometric factor

I = Current (ampere)

Apparent resistivity is defined as the calculated subsurface resistivity which indicates the resistivity of a homogeneous ground with the same resistance value for the same electrode array. The apparent resistivity has a complex relationship with true resistivity value. To calculate the true resistivity value of the subsurface, the apparent resistivity value is used. While the inversion process needs to be applied for apparent resistivity by using a computer program in identifying true subsurface resistivity, (Ismail, 2015). Figure 3.5 shows a basic resistivity measurement using four electrodes arrangement to determine apparent resistivity,  $\rho_a$  for ground subsurface.

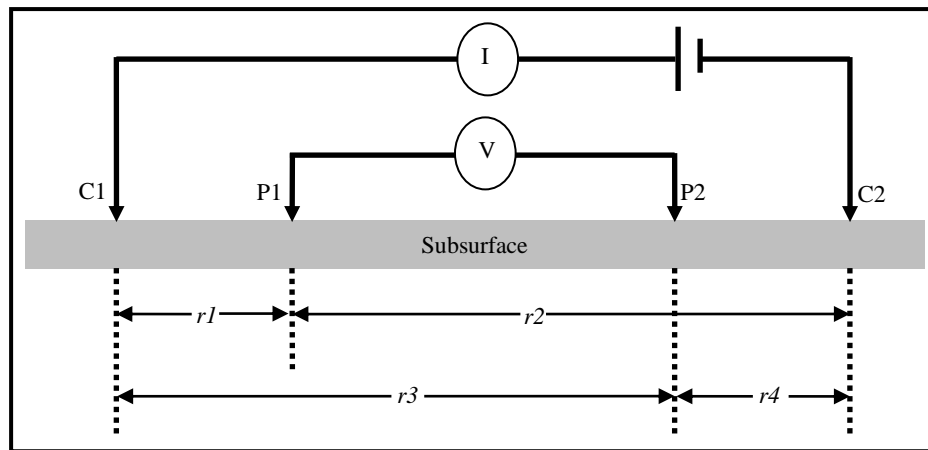


Figure 3.5: Basic current and potential electrodes arrangement in electrical resistivity method (modified after Telford et al., 1990).

The current electrode, C1 is assumed as positive current electrode (source) and C2 as negative current electrode (sink). The detection of potential value at P1 due to the source, C1 is written as;  $+\rho_a I/(2\pi r1)$ , while potential value at P2 due to the sink, C2 is written as;  $-\rho_a I/(2\pi r4)$ . The combined potential at P1 is given by Equation 3.5-3.7.